

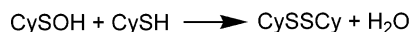
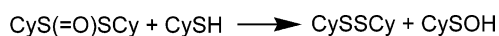
Reactive Sulfur Species: Kinetics and Mechanisms of the Reaction of Cysteine Thiosulfinate Ester with Cysteine to Give Cysteine Sulfenic Acid

Péter Nagy, Kelemu Lemma, and Michael T. Ashby*

Department of Chemistry and Biochemistry, University of Oklahoma, Norman, Oklahoma 73019

mashby@ou.edu

Received August 17, 2007



The kinetics and mechanisms of the reaction of cysteine with cysteine thiosulfinate ester in aqueous solution have been studied by stopped-flow spectrophotometry between pH 6 and 14. Two reaction pathways were observed for pH > 12: (1) an essentially pH-independent nucleophilic attack of cysteine on cysteine thiosulfinate ester, and (2) a pH-dependent fast equilibrium protonation of cysteine sulfenate that is followed by rate-limiting comproportionation of cysteine sulfenic acid with cysteine to give cystine. For 6 < pH < 12, the rate-determining reaction between cysteine and cysteine thiosulfinate ester becomes pH-dependent due to the protonation of their amine groups. Hydrolysis of cysteine thiosulfinate ester does not play a role in the aforementioned mechanisms because the rate-determining nucleophilic attack by hydroxide is relatively slow.

Introduction

It had been long recognized that cysteine (CySH)¹ residues in proteins can be “over-oxidized” beyond the disulfide form under conditions of oxidative stress.² More recently, evidence has been introduced for functional protein sulfenic acid moieties for native proteins, such as NADH peroxidase,³ NADH oxidase,⁴ nitrile hydratase,⁵ both classes of methionine sulfoxide reductases,⁶ and certain peroxiredoxins.^{7–11} However, in contrast to the relatively stable sulfenic derivatives of cysteine that have

been identified in proteins, the parent compound remains elusive. In fact, of the common oxidized derivatives of cysteine (Scheme 1), only cysteine sulfenic acid (CySOH) has not been isolated. With the exception of a few derivatives that are stabilized through steric hindrance, H-bonding, or conjugation,^{12–17} sulfenic acids are generally considered to be transient species.¹⁸ One reason that CySOH exhibits only fleeting existence is that its condensation to give the corresponding cysteine thiosulfinate ester, CyS(=O)SCy, is a facile process:



The CySOH/CyS(=O)SCy equilibrium is unique among acid/anhydride equilibria in that the anhydride is thermodynamically

(1) References to compounds without charges are inclusive of all acid/base derivatives. Specific proton states are referenced in the Discussion section and some of the schemes.

(2) Allison, W. S. *Acc. Chem. Res.* **1976**, *9*, 293–299.

(3) Yeh, J. I.; Claiborne, A. *Methods Enzymol.* **2002**, *353*, 44–54.

(4) Mallett, T. C.; Parsonage, D.; Claiborne, A. *Biochemistry* **1999**, *38*, 3000–3011.

(5) Endo, I.; Nojiri, M.; Tsujimura, M.; Nakasako, M.; Nagashima, S.; Yohda, M.; Odaka, M. *J. Inorg. Biochem.* **2001**, *83*, 247–253.

(6) Boschi-Muller, S.; Olry, A.; Antoine, M.; Branlant, G. *Biochim. Biophys. Acta* **2005**, *1703*, 231–238.

(7) Claiborne, A.; Yeh, J. I.; Mallett, T. C.; Luba, J.; Crane, E. J., III; Charrier, V.; Parsonage, D. *Biochemistry* **1999**, *38*, 15407–15416.

(8) Claiborne, A.; Miller, H.; Parsonage, D.; Ross, R. P. *FASEB J.* **1993**, *7*, 1483–1490.

(9) Van den Broek, L. A. G. M.; Delbressine, L. P. C.; Ottenheijm, H. C. J. Biochemistry and metabolic pathways of sulfenic acids and their derivatives. In *The Chemistry of Sulphenic Acids and Their Derivatives*; Patai, S., Ed.; John Wiley: New York, 1990; pp 701–721.

(10) Claiborne, A.; Mallett, T. C.; Yeh, J. I.; Luba, J.; Parsonage, D. *Adv. Protein Chem.* **2001**, *58*, 215–276.

(11) Jeong, W.; Park, S. J.; Chang, T.-S.; Lee, D.-Y.; Rhee, S. G. *J. Biol. Chem.* **2006**, *281*, 14400–14407.

(12) Goto, K.; Shimada, K.; Furukawa, S.; Miyasaka, S.; Takahashi, Y.; Kawashima, T. *Chem. Lett.* **2006**, *35*, 862–863.

(13) Goto, K.; Holler, M.; Okazaki, R. *J. Am. Chem. Soc.* **1997**, *119*, 1460–1461.

(14) Ishii, A.; Komiya, K.; Nakayama, J. *J. Am. Chem. Soc.* **1996**, *118*, 12836–12837.

(15) Tripolt, R.; Belaj, F.; Nachbaur, E. *Z. Naturforsch., B: Chem. Sci.* **1993**, *48*, 1212–1222.

(16) Yoshimura, T.; Tsukurimichi, E.; Yamazaki, S.; Soga, S.; Shimasaki, C.; Hasegawa, K. *Chem. Commun.* **1992**, 1337–1338.

(17) Nakamura, N. *J. Am. Chem. Soc.* **1983**, *105*, 7172–7173.

(18) Patai, S. *The Chemistry of Sulphenic Acids and Their Derivatives*; John Wiley: New York, 1990.

SCHEME 1. Nomenclature and Oxidation States of Common Derivatives of Cysteine

	CySH	CySOH	CySO ₂ H	CySO ₃ H
ox state	-2	0	+2	+4
name	thiol	sulfenic acid	sulfinic acid	sulfonic acid
ox state	-1/-1	+1/-1	+3/-1	
name	disulfide	thiosulfinate ester	thiosulfonate ester	

favored over the acid. In an attempt to probe the reaction chemistry of CySOH, we have recently investigated the kinetics and mechanisms of the hydrolysis of CyS(=O)SCy. However, for pH < 13, the hydrolysis reaction is slower than the subsequent reactions of CySOH. In the present study, we describe the kinetics of the reaction of CySH with CyS(=O)SCy between pH 6 and 14. Below pH 12, the nucleophilic attack of CySH on the electrophilic CyS(=O)SCy is rate-limiting. However, above pH 12, in the presence of excess CySH, the subsequent comproportionation of CySOH with CySH becomes rate-limiting. Thus, the title reaction affords what is apparently the first detailed mechanistic study of a reaction of CySOH.

Results

Products of the Reaction of CyS(=O)SCy with CySH. The only product of the reaction of CySH with CyS(=O)SCy that is observed by ¹H NMR under the conditions of all of the kinetic experiments that are discussed herein is CySSCy. Thus, hydrolysis of CyS(=O)SCy and its subsequent reactions (which would result in the formation of cysteine sulfinic acid, CySO₂H)¹⁹ are not competitive with the reactions that we consider here, even at pH 14. It is noteworthy that CySSCy is also subject to hydrolysis at high pH. For example, at pH 14, it decomposes to give a mixture of CySH and CySO₂H (and a yellow product that is silent in the ¹H NMR or is a minor species). However,

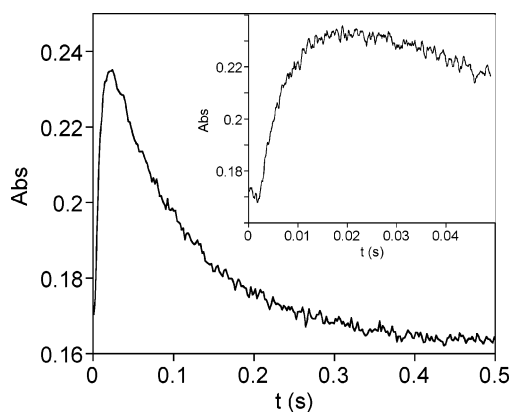


FIGURE 1. Observed kinetic traces at $\lambda = 300$ nm. Conditions: $[\text{CyS}(=\text{O})\text{SCy}]_0 = 1.25$ mM, $[\text{CySH}] = 25$ mM, $[\text{OH}^-] = 0.095$ M, $I = 1.0$ M (NaClO₄ + NaOH), $T = 18$ °C.

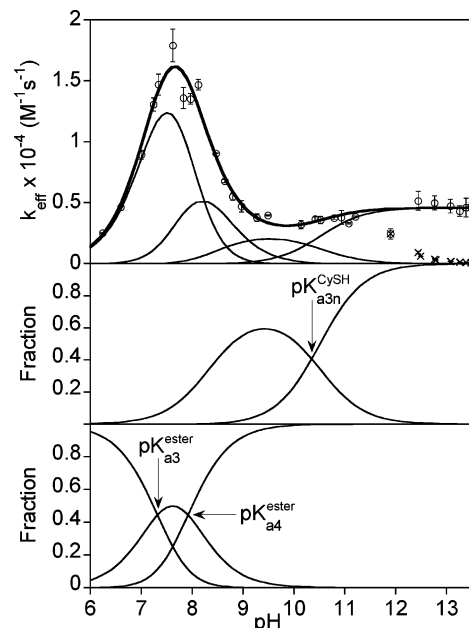


FIGURE 2. Effect of pH on the kinetics of the reaction of CyS(=O)SCy with CySH. The kinetic traces were measured at $\lambda = 268$ nm and fit to a single-exponential function below pH 12. Above pH 12, the kinetic traces were measured at $\lambda = 300$ nm and fit to double-exponential functions. One of the exponential functions was pH-independent (circles and bold line), and the other function increased with decreasing pH (crosses). The data point at ca. pH 12 (illustrated with both a circle and a cross) was fit with a single exponential function, but it is certainly a composite of the two functions. Conditions: For the data at pH > 12, combination of two sets of data (1) $[\text{CyS}(=\text{O})\text{SCy}]_0 = 1.25$ mM, $[\text{CySH}] = 25$ mM, $[\text{OH}^-] = 0.05\text{--}0.5$ M, $I = 1.0$ M (NaClO₄ + NaOH), $T = 18$ °C; (2) $[\text{CyS}(=\text{O})\text{SCy}]_0 = 125$ μM , $[\text{CySH}] = 2.5$ mM, $[\text{OH}^-] = 0.05\text{--}0.5$, $I = 1.0$ M (NaClO₄ + NaOH), $T = 18$ °C. For the data at pH < 12, $[\text{CyS}(=\text{O})\text{SCy}]_0 = 125$ μM , $[\text{CySH}] = 2.5$ mM, pH = 10–12, iP or Tris = 0.1 M, $I = 1.0$ M (NaClO₄ + iP/Tris), $T = 18$ °C. Top: computed k_{eff} (using eq 9) for the $k_{1b} = 4.7(2) \times 10^5$ M⁻¹ s⁻¹ pathway, $k_{1b'} = 5.7(6) \times 10^4$ M⁻¹ s⁻¹ pathway, $k_{1b''} = 3.6(7) \times 10^3$ M⁻¹ s⁻¹ pathway, $k_{1b'''} = 4.6(3) \times 10^3$ M⁻¹ s⁻¹ pathway, and combined $k_{1b} + k_{1b'} + k_{1b''} + k_{1b'''}$ pathways (individual pathway contributions illustrated together with the summation in bold) at 18 °C. The observed k_{eff} (circles and crosses) with standard deviations (as error bars) are also plotted. Middle: computed speciation of CyS^- and CyS^{2-} for $\text{p}K_{a2s}^{\text{CySH}} = 8.5$, $\text{p}K_{a2n}^{\text{CySH}} = 8.9$, $\text{p}K_{a3s}^{\text{CySH}} = 10.0$, and $\text{p}K_{a3n}^{\text{CySH}} = 10.4$. The point at which $[\text{CyS}^-] = [\text{CyS}^{2-}]$ is $\text{p}K_{a3n}^{\text{CySH}}$ (shown). Bottom: computed speciation of $\text{CyS}(=\text{O})\text{SCy}^0$, $\text{CyS}(=\text{O})\text{SCy}^-$, and $\text{CyS}(=\text{O})\text{SCy}^{2-}$ for $\text{p}K_{a3}^{\text{ester}} = 7.3$ and $\text{p}K_{a4}^{\text{ester}} = 7.9$.

this decomposition process is slow, even at very high pH (e.g., the extent of decomposition at pH 14 is only 10% after 5 days). Accordingly, although CySSCy is not thermodynamically stable at high pH, it is a long-lived intermediate that is readily characterized before its decomposition.

Kinetics of the Reaction of CyS(=O)SCy with CySH at pH Higher than 12. The reaction of CyS(=O)SCy with excess CySH can be modeled with a single-exponential between pH 6 and 12 (vide infra), but a double-exponential function is required to model the absorption traces above pH 12 (Figure 1). The first exponential function corresponds to the reaction that is observed below pH 12 (vide infra). Above pH 12, this reaction is essentially pH-independent (although it becomes pH-depend-

(19) Nagy, P.; Ashby, M. T. *Chem. Res. Toxicol.* **2007**, *20*, 1364–1372.

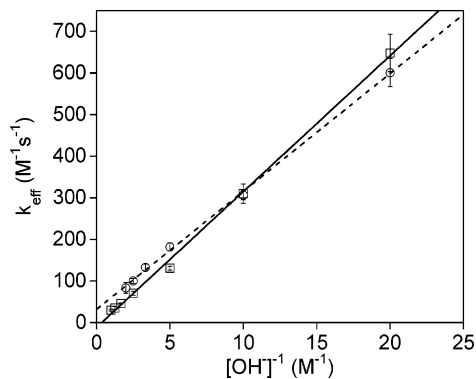


FIGURE 3. The $[\text{OH}^-]^{-1}$ dependency of the reaction of CySOH with CySH, where CySOH was generated in situ by the reaction of CyS(=O)SCy with CySH (circles) or the reaction of HOX (X = Cl, Br) with CySH (squares). Kinetic traces were collected at $\lambda = 268$ nm. The dashed line (slope = $28.3(5) \text{ s}^{-1}$ and intercept = $32(5) \text{ M}^{-1} \text{ s}^{-1}$) and solid line (slope = $32.6(7) \text{ s}^{-1}$ and intercept = $-12(6) \text{ M}^{-1} \text{ s}^{-1}$) represent least-squares fits for the circle and square data, respectively. Conditions: circles: $[\text{CyS(=O)SCy}]_0 = 125 \mu\text{M}$, $[\text{CySH}] = 2.5 \text{ mM}$, $[\text{OH}^-] = 0.05\text{--}0.5 \text{ M}$, $I = 1.0 \text{ M}$ (NaClO₄ + NaOH), $T = 18 \text{ }^\circ\text{C}$; squares: $[\text{OCl}^-]_0 = 50 \mu\text{M}$, $[\text{CySH}] = 0.5 \text{ mM}$, $[\text{OH}^-] = 0.05\text{--}1 \text{ M}$, $I = 1.0 \text{ M}$ (NaClO₄ + NaOH), $T = 18 \text{ }^\circ\text{C}$.

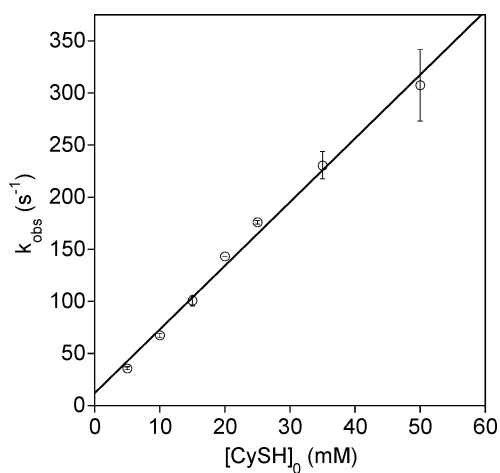


FIGURE 4. Effect of $[\text{CySH}]$ on the reaction of CyS(=O)SCy with CySH. Kinetic traces were collected at $\lambda = 300$ nm. Conditions: $[\text{CyS(=O)SCy}]_0 = 1 \text{ mM}$, $[\text{CySH}]_0 = 5\text{--}50 \text{ mM}$, $[\text{OH}^-] = 0.5 \text{ M}$, $I = 1.0 \text{ M}$ (NaClO₄ and NaOH), $T = 18 \text{ }^\circ\text{C}$.

ent below pH 12, vide infra). The second exponential function yields pseudo-first-order rate constants (k_{obs}) that exhibit a pH dependency. The effective rate constant ($k_{\text{eff}} = k_{\text{obs}}/[\text{CySH}]_0$) for the two reactions that are observed above pH 12 is illustrated in Figure 2 as a function of pH. The plots of k_{eff} for the slower reaction versus $1/[\text{OH}^-]$ for $\text{pH} > 12$ can be modeled with a straight line that passes through the origin (Figure 3, circles and dashed line). The reaction that corresponds to the first exponential function (Figure 4) and the more pH-dependent reaction that corresponds to the second exponential function (Figure 5) both exhibit first-order dependencies on $[\text{CySH}]$. Thus, the first reaction exhibits overall second-order kinetics between pH 12 and 14 (first-order each in $[\text{CyS(=O)SCy}]$ and $[\text{CySH}]$), and the second reaction exhibits third-order kinetics between pH 12 and 14 (first-order each in [oxidized cysteine intermediate], $[\text{CySH}]$, and $[\text{H}^+]$).

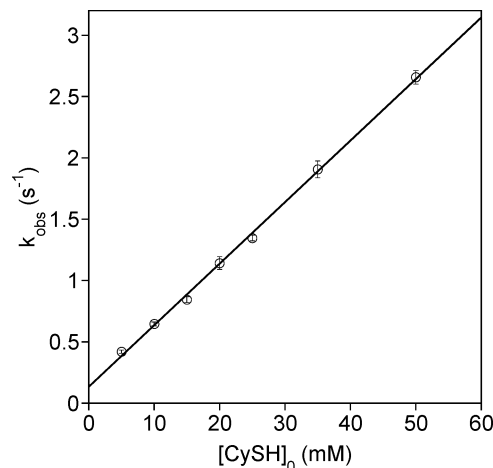
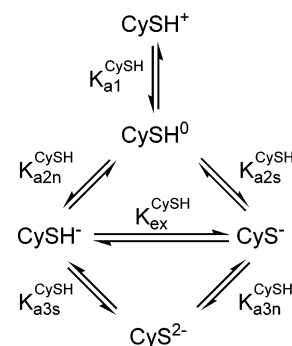


FIGURE 5. Effect of $[\text{CySH}]$ on the reaction of CySOH with CySH. Kinetic traces were collected at $\lambda = 300$ nm. Conditions: $[\text{CyS(=O)SCy}]_0 = 1 \text{ mM}$, $[\text{CySH}]_0 = 5\text{--}50 \text{ mM}$, $[\text{OH}^-] = 0.5 \text{ M}$, $I = 1.0 \text{ M}$ (NaClO₄ and NaOH), $T = 18 \text{ }^\circ\text{C}$.

SCHEME 2. Acid/Base Equilibria for CySH



Kinetics of the Reaction of CyS(=O)SCy with CySH between pH 6 and 12. The reaction can be modeled with a single exponential for $6 < \text{pH} < 12$. The observed rate constants show a first-order dependency on $[\text{CySH}]$ (investigated at pH 4.5, 6.2, 8.2, and 10.7, data not shown). A plot of k_{eff} versus pH in this pH range exhibits bell-shaped behavior with a maximum at pH 7.7, which indicates that multiple reaction pathways are operating (Figure 2).

Discussion

Protonation States of the Redox Derivatives of CySH and CyS(=O)SCy. The reactions that are described herein have been studied over a range of pH that spans several acid dissociations. The protonation states of the reaction partners can have profound effects on the rate of a reaction. In some cases, the effect is readily rationalized (e.g., a thiolate is a better nucleophile than a thiol). Up to this point, references to compounds without charges have been inclusive of all of the protonation states of the species (e.g., CySH). However, it will become necessary later to refer to specific protonation states when we model the kinetic data. Importantly, for polyprotic acids that exhibit closely spaced pK_a values, it is not possible to assign the macroscopic acid dissociation constants to a microscopic pK_a (i.e., to the dissociation of proton from a specific functional group).²⁰ CySH exhibits three macroscopic acid dissociations and five micro-

(20) Bodner, G. M. *J. Chem. Educ.* **1986**, *63*, 246–247.

scopic acid dissociations (Schemes 2 and 3), although the first acid dissociation (K_{a1}^{CySH}) is outside the scope of the pH range of this study, $6 < \text{pH} < 14$. Hence, there are four microscopic protonation states for CySH between pH 6 and 14 for $I = 1.0$ and 25°C that are relevant here (Schemes 2 and 3):^{20–33}

$$K_{a2s}^{\text{CySH}} = \frac{[\text{CyS}^-][\text{H}^+]}{[\text{CySH}^0]} = 3.2(3) \times 10^{-9} \text{ M} \quad (2)$$

$$K_{a2n}^{\text{CySH}} = \frac{[\text{CySH}^-][\text{H}^+]}{[\text{CySH}^0]} = 1.4(1) \times 10^{-9} \text{ M} \quad (3)$$

$$K_{a3s}^{\text{CySH}} = \frac{[\text{CyS}^{2-}][\text{H}^+]}{[\text{CySH}^-]} = 1.0(1) \times 10^{-10} \text{ M} \quad (4)$$

$$K_{a3n}^{\text{CySH}} = \frac{[\text{CyS}^{2-}][\text{H}^+]}{[\text{CyS}^-]} = 4.5(5) \times 10^{-11} \text{ M} \quad (5)$$

The following equations relate the macroscopic and microscopic acid dissociation constants:

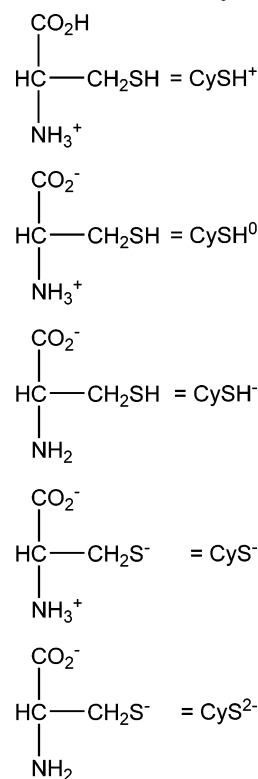
$$K_{a2}^{\text{CySH}} = K_{a2s}^{\text{CySH}} + K_{a2n}^{\text{CySH}} = \frac{\{[\text{CyS}^-] + [\text{CySH}^-]\}[\text{H}^+]}{[\text{CySH}^0]} \quad (6)$$

$$K_{a3}^{\text{CySH}} = \frac{K_{a3s}^{\text{CySH}}K_{a3n}^{\text{CySH}}}{K_{a3s}^{\text{CySH}} + K_{a3n}^{\text{CySH}}} = \frac{[\text{CyS}^{2-}][\text{H}^+]}{[\text{CyS}^-] + [\text{CySH}^-]} \quad (7)$$

We have confirmed the previously reported^{20,21} macroscopic acid dissociation constants for CySH at $I = 1.0 \text{ M}$ and 25°C by spectral titration followed by deconvolution of the pH-dependent spectra using singular value decomposition (SVD) analysis: $\text{p}K_{a2}^{\text{CySH}} = 8.1$ and $\text{p}K_{a3}^{\text{CySH}} = 10.1$. These macroscopic acid dissociation constants are comparable to those that are calculated from the relationships of eqs 6 and 7, $\text{p}K_{a2}^{\text{CySH}} = 8.3$ and $\text{p}K_{a3}^{\text{CySH}} = 10.5$. We will show later that the thiolate forms of CySH (CyS^- and CyS^{2-}) are most reactive toward CyS(=O)SCy .

For CyS(=O)SCy , we have previously shown that the two ammonium groups are deprotonated essentially independently, although a statistical factor of $\log(4)$ presumably separates the macroscopic acid dissociation constants.¹⁹ Since the ammonium

SCHEME 3. Protonation States for CySH



acid dissociations are the only ones for CyS(=O)SCy that fall within the range of pH 6 and 14, there are three relevant macroscopic proton states: CyS(=O)SCy^0 , CyS(=O)SCy^- , and CyS(=O)SCy^{2-} . In principle, since the ester is unsymmetrical with respect to its two amine groups, CyS(=O)SCy^- should exist in two microscopic protonation states. However, because the macroscopic $\text{p}K_a$ values for CyS(=O)SCy^{x-} ($x = 0-2$) are essentially the same, it follows that the two microscopic protonation states of CyS(=O)SCy^- are equally populated. For the sake of simplicity, we will only refer to the macroscopic protonation state of CyS(=O)SCy^- during this discussion. The protonation state of CySOH is of course also relevant to the discussion, but unlike the other derivatives of CySH that are given in Scheme 1, its acid dissociation constants are unknown (vide infra).

Possible Elementary Redox Reactions of CySH and its Redox Derivatives. For the five species of Scheme 1 that are under consideration, it can be shown that there are four possible nondegenerate bimolecular elementary reactions of CyS(=O)SCy (Scheme 4, **1a–d**). Furthermore, there are four possible nondegenerate bimolecular elementary reactions of CySOH . Three of the reactions of CySOH involve CyS(=O)SCy (Scheme 4, **-1a, -1b, and 1d**). The fourth reaction of CySOH is its comproportionation with CySH to give CySSCy (Scheme 4, **2**). Importantly, when we refer to these reactions by number (**1a–d** and **2**) throughout the remainder of this discussion, we are not referencing any particular acid/base state of the reactants and products (as many of the reactions are expected to exhibit multiple proton states that may affect the kinetics of a given reaction). The proton states will be specifically referenced when the mechanisms are discussed later.

Relevant Elementary Redox Reactions. This study is focused on reaction **1b** and its subsequent reaction **2** (Scheme 4). However, it is important to address the relevance of the other

(21) Benesch, R. E.; Benesch, R. *J. Am. Chem. Soc.* **1955**, *77*, 5877–5881.

(22) Grunwald, E.; Chang, K. C.; Skipper, P. L.; Anderson, V. K. *J. Phys. Chem.* **1976**, *80*, 1425–1431.

(23) Stricks, W.; Koltzoff, I. M. *J. Am. Chem. Soc.* **1951**, *73*, 4569–4574.

(24) De Deken, R. H.; Broekhuysen, J.; Bechet, J.; Mortier, A. *Biochim. Biophys. Acta* **1956**, *19*, 45–52.

(25) Reuben, D. M. E.; Bruce, T. C. *J. Am. Chem. Soc.* **1976**, *98*, 114–121.

(26) Elson, E. L.; Edsall, J. T. *Biochemistry* **1962**, *1*, 1–7.

(27) Edsall, J. T.; Martin, R. B.; Hollingworth, B. R. *Proc. Natl. Acad. Sci. U.S.A.* **1958**, *44*, 505–518.

(28) Edsall, J. T. *Biochemistry* **1965**, *4*, 28–31.

(29) Gorin, A. I.; Serebrianyi, A. M.; Zoz, N. N.; Kharitonov, I. G.; Slavenas, I.; Atkociunaite, V.; Antonova, L. V.; Tseitlin, P. I. *Byull. Eksp. Biol. Med.* **1976**, *81*, 425–427.

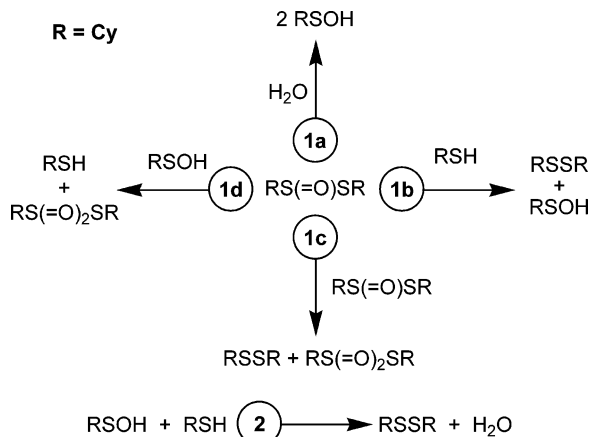
(30) Serebrianyi, A. M.; S'lakste, N. I.; Gorin, A. I.; Tseitlin, P. I.; Bogomolova, N. S. *Byull. Eksp. Biol. Med.* **1983**, *96*, 84–86.

(31) Connett, P. H.; Wetterhahn, K. E. *J. Am. Chem. Soc.* **1986**, *108*, 1842–1847.

(32) Szakacs, Z.; Krasnzi, M.; Noszal, B. *Anal. Bioanal. Chem.* **2004**, *378*, 1428–1448.

(33) Hegedus, H.; Gergely, A.; Horvath, P.; Noszal, B. *J. Chem. Res.* **1999**, *306–307*, 1331–1342.

SCHEME 4. Possible Elementary Bimolecular Redox Reactions of Cysteine Thiosulfinate Ester (1a–d) and Cysteine Sulfinic Acid (-1a, -1b, 1d, and 2)



possible elementary reactions of redox derivatives of CySH. As mentioned before, CySO_2H and cysteine sulfonic acid (CySO_3H) were not observed as products under the conditions of our experiments. Furthermore, since CySO_2H and CySO_3H were found to be relatively inert toward the five CySH derivatives that are considered herein (data not shown), they have not been included as possible intermediates in the reactions that are the subject of this study. We have shown in a previous study¹⁹ that both the hydrolysis of $\text{CyS(=O)}_2\text{SCy}$ and its reaction with CySH result in the formation of CySO_2H (and that $\text{CyS(=O)}_2\text{SCy}$ does not react with CySSCy). So, the possible elementary reactions **1c** and **1d** can be eliminated from our models. In the same study, we have reported the detailed kinetics of reaction **1a**.¹⁹ Reaction **1b** is kinetically incompetent since it is apparent that reaction **1b** is at least 100 times faster than reaction **1a** under all the experimental conditions used here. The possible relevance of reactions **-1a** and **-1b** will be considered next.

With respect to reaction **-1b**, the effect of $[\text{CySSCy}]$ on the reactions of CySH with CyS(=O)SCy and CySOH was studied by double-mixing stopped-flow spectroscopy (data not shown). The rates of these reactions were found to be independent of $[\text{CySSCy}]$, even at relatively high CySSCy concentrations, which suggest that reaction **-1b** is not relevant to this study.

In order to investigate the possible relevance of reaction **-1a**, we devised the double-mixing experiments of Figure 6 wherein the elementary hydrolysis step of CyS(=O)SCy (Sequence A), a reaction that produces either 1 molar equiv of CySO_2H and CySH or 2 molar equiv of CySOH (reaction **1a**),¹⁹ was allowed to compete with the reaction of CyS(=O)SCy with 1 molar equiv of CySH (Sequence B), a reaction that produces 1 molar equiv of CySOH (reaction **1b**). At pH 13, mixing Sequence A of Figure 6 (in the absence of added CySH) results in a first-order kinetic trace (Figure 7, dashed line) with a rate constant that is similar to the one measured for the hydrolysis of CyS(=O)SCy under these conditions.¹⁹ In contrast, when 1 molar equiv of CySH was introduced in the second mixing cycle after a delay time of 20 ms (Figure 6, Sequence B), a second-order kinetic trace was observed following the rapid reaction of CyS(=O)SCy with CySH (Figure 7, solid line). We interpret this event as either the disproportionation (that results in 1 molar equiv of CySH and 1 molar equiv of CySO_2H) or the condensation of 2 molar equiv of CySOH (reaction **-1a**). In order to obtain clean second-order kinetic traces, $[\text{CyS(=O)SCy}]_0 =$

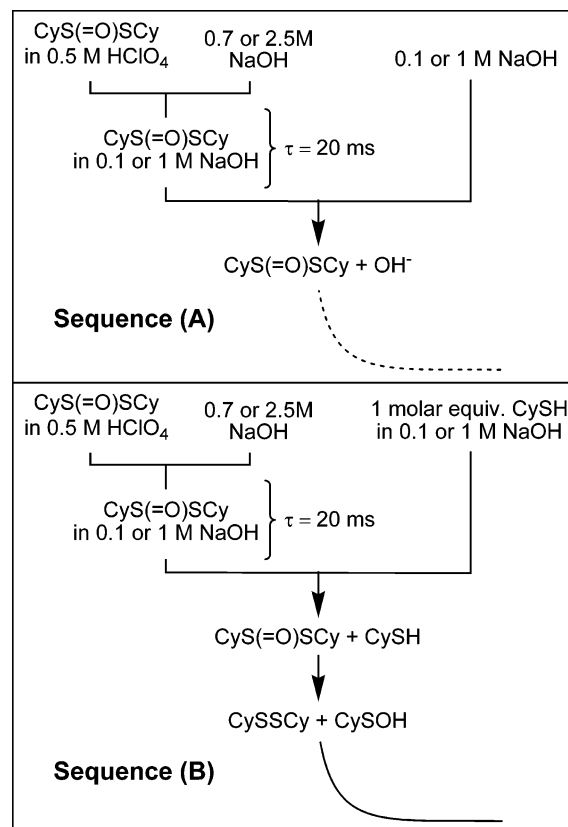


FIGURE 6. Double-mixing sequences that produced the kinetic traces of Figures 7 and 8 (Sequence A produced the dashed traces, and Sequence B produced the solid traces).

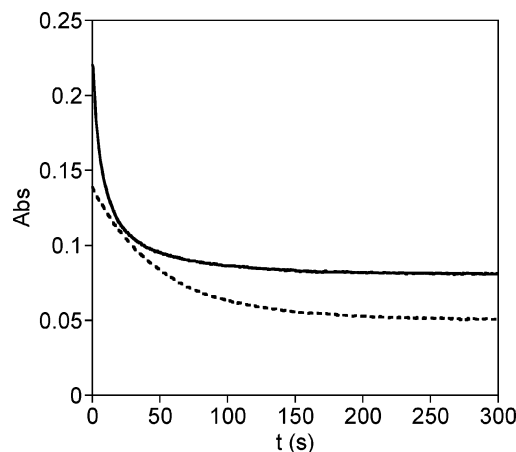
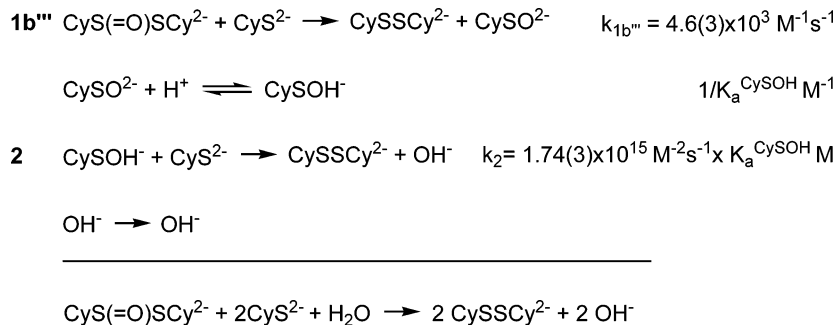


FIGURE 7. Kinetic traces of the hydrolysis of CyS(=O)SCy (dashed line) and the disproportionation/condensation of CySOH (solid line) at pH 13 and $\lambda = 260$ nm. Conditions: hydrolysis: $[\text{CyS(=O)SCy}]_0 = 0.125$ mM, pH = 13, and $I = 1.0$ M ($\text{NaClO}_4 + \text{NaOH}$); disproportionation/condensation: $[\text{CyS(=O)SCy}]_0 = 0.125$ mM, $[\text{CySH}]_0 = 0.125$ mM, pH = 13, and $I = 1.0$ M ($\text{NaClO}_4 + \text{NaOH}$), $T = 18$ °C.

$[\text{CySH}]_0$ had to be kept below 250 μM . At higher initial concentrations, biphasic kinetic traces were observed (following the rapid reaction of CyS(=O)SCy with CySH) where a fast second-order process is followed by a slower first-order process. The rate constants of the second-order process correspond to the second-order process that is measured at lower concentrations of the reactants ($[\text{CyS(=O)SCy}]_0 = [\text{CySH}]_0$). The rate

SCHEME 5. Proposed Mechanism, Equilibrium, and Rate Constants (at 18 °C) for the Reaction of CyS(=O)SCy²⁻ and CyS²⁻ under Alkaline Conditions


constant of the subsequent first-order reaction corresponds to the hydrolysis of CyS(=O)SCy. The relative absorbance change throughout the slow first-order process increased with increasing concentrations of the reactants ($[\text{CyS(=O)SCy}]_0 = [\text{CySH}]_0$). This observation indicates that the condensation of 2 molar equiv of CySOH to give the CyS(=O)SCy (reaction **-1a**) is faster or at least competitive with the disproportionation of two CySOH at pH 13. We have repeated the double-mixing experiment of Figure 6 at pH 14 (Figure 8). When CySH was introduced in the second mixing cycle at pH 14 (Sequence B), a second-order trace was observed with a rate constant that is a factor of 2 smaller than the one that was obtained in the corresponding experiment at pH 13. In the absence of added CySH (Sequence A), complex kinetic traces were observed. Polychromatic data suggest that one or more reactions of CySOH (disproportionation and/or the condensation) are competitive with the hydrolysis of CyS(=O)SCy at pH 14 (under the experimental conditions of Sequence A). On the basis of the calculated rate constants of the second-order reactions (Sequence B), we conclude that reaction **-1a** is not competitive with the reaction of CySH and CySOH at pH 13 and reaction **-1a** is only a minor reaction pathway at pH 14. A detailed discussion of the mechanism of the reaction of CySOH with itself (i.e., condensation and/or disproportionation) is outside the scope of the present study.

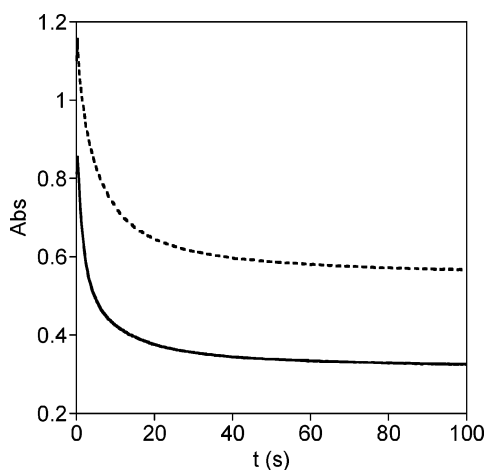


FIGURE 8. Kinetic traces of the hydrolysis of CyS(=O)SCy (dashed line) and the disproportionation/condensation of CySOH (solid line) at pH 14 and $\lambda = 260$ nm. Conditions: hydrolysis: $[\text{CyS(=O)SCy}]_0 = 1$ mM, pH = 14, and $I = 1.125$ M (0.125 M NaClO₄ + 1.0 M NaOH); disproportionation/condensation: $[\text{CyS(=O)SCy}]_0 = 1$ mM, $[\text{CySH}]_0 = 1$ mM, pH = 14, and $I = 1.125$ M (0.125 M NaClO₄ + 1.0 M NaOH), $T = 18$ °C.

Kinetics of the Reactions of CyS(=O)SCy with CySH at pH Higher than 12. We interpret the results of Figures 1–5 in terms of the mechanism that is outlined in Scheme 5. The faster, largely pH-independent reaction that is observed between pH 12 and 14 is attributed to reaction **1b**, where a value of $k_{1b}''' = 4.0(8) \times 10^3 \text{ M}^{-1} \text{ s}^{-1}$ was calculated by averaging six values of k_{eff} that were measured between pH 12.4 and 13.5. Essentially the same value of k_{1b}''' is obtained for a more complete rate law that encompasses all of the kinetic data we have collected between pH 6 and 14 (vide infra).

The pH-dependent data for the slower reaction of Figure 2 that were observed between pH 12 and 14 (the data that lie below the bold line, vide supra) correspond to the same rate data for the reactions of HOX (X = Cl or Br) with CySH that are observed between pH 12 and 14.³⁴ Figure 3 demonstrates that both sets of data can be fit to the same linear function with respect to $1/[\text{OH}^-]$ to give essentially the same slope and intercept. We have interpreted the pH dependency of these kinetic data in the context of a fast pre-equilibrium protonation of cysteine sulfenate (that is produced in the preceding reaction, **1b**) to give the sulfenic acid, followed by rate-limiting disproportionation of sulfenic acid and cysteinylate (Scheme 5). CySH is completely deprotonated above pH 12 (i.e., CyS^{2-}). In a recent parallel study (vide infra), we have shown that CySOH is also completely deprotonated above pH 12 (i.e., CySO^{2-}).³⁴ Accordingly, the first-order dependency of the reaction on $[\text{H}^+]$ (or $1/[\text{OH}^-]$) that is evidenced in Figure 3 implies that the sulfenate moiety is protonated by a single proton (i.e., CySOH^- , as two protons to produce CySOH^0 as the intermediate would result in a second-order dependency on $[\text{H}^+]$ for the reaction of CyS^{2-} and CySO^{2-}). However, the data are also consistent with the reaction of the sulfenate with the thiol. We note that it has been previously proposed that the peroxy-nitrate anion reacts with thiols.^{35,36} However, our attribution of the reaction to CyS^{2-} is consistent with the general consensus that sulfenic acids are good electrophiles and thiolates are good nucleophiles. The linear relationship of these kinetic data and the fact that the curve-fitting line in Figure 3 passes through the origin suggests that the reaction between pH 12 and 14 is occurring well above the acid dissociation constant of CySOH^- ($\text{p}K_a^{\text{CySOH}}$). Although CySO^{2-} is apparently the dominant species, we conclude it exhibits undetectable reactivity, and CySOH^- is instead the reaction partner of CyS^{2-} between pH

(34) Nagy, P.; Ashby, M. T. *J. Am. Chem. Soc.* **2007**, submitted.

(35) Radi, R.; Beckman, J. S.; Bush, K. M.; Freeman, B. A. *J. Biol. Chem.* **1991**, *266*, 4244–4250.

(36) Quijano, C.; Alvarez, B.; Gatti, R. M.; Augusto, O.; Radi, R. *Biochem. J.* **1997**, *322*, 167–173.

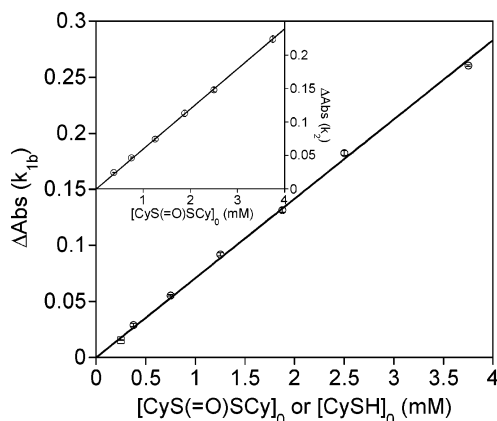


FIGURE 9. Circles: Effect of $[\text{CyS(=O)SCy}]_0$ on the change in absorbance, ΔAbs , for the reaction of CyS(=O)SCy with CySH and the reaction of CySOH with CySH (inset) when CyS(=O)SCy and CySOH are the limiting reagents, respectively. Square: Effect of $[\text{CySH}]_0$ on the change in absorbance, ΔAbs , for the pH-independent reaction that is observed between CyS(=O)SCy and CySH when CySH is the limiting reagent. Kinetic traces were collected at $\lambda = 300$ nm. Conditions: circles: $[\text{CyS(=O)SCy}]_0 = 0.375\text{--}3.75$ mM, $[\text{CySH}] = 25$ mM, $[\text{OH}^-] = 0.1$ M, $I = 1.0$ M (NaClO_4 and NaOH), $T = 18$ °C; square: $[\text{CyS(=O)SCy}]_0 = 1$ mM, $[\text{CySH}]_0 = 0.25$ mM, $[\text{OH}^-] = 0.1$ M, $I = 1.0$ M (NaClO_4 and NaOH), $T = 18$ °C.

12 and 14. Since pK_a^{CySOH} cannot be determined from these data, the rate law is given by

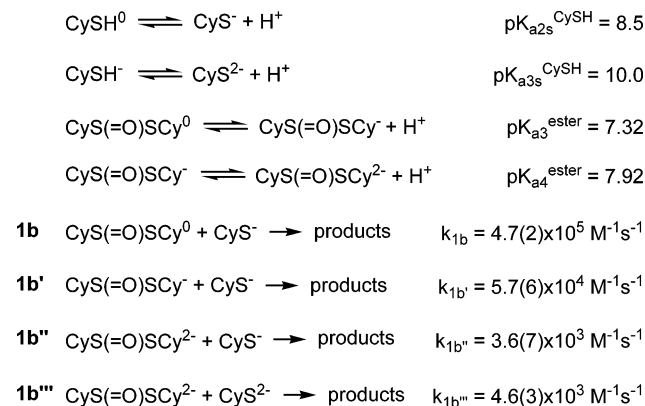
$$\text{rate} = \frac{-d[\text{CySOH}^-]}{dt} = k_2[\text{CyS}^{2-}][\text{CySOH}^-] = \frac{k_2}{K_a^{\text{CySOH}}} [\text{H}^+][\text{CySH}]_T[\text{CySOH}]_T \quad (8)$$

where the protonation states are defined in Scheme 2. On the basis of the fit in Figure 3 (dashed line), we have determined that $k_2 = (1.74(3) \times 10^{15} \text{ M}^{-2} \text{ s}^{-1}) \times (K_a^{\text{CySOH}} \text{ M})$.

To further support the proposed mechanism (Scheme 5), we have investigated the effect of $[\text{CyS(=O)SCy}]_0$ on the observed absorbance change throughout the two consecutive reactions that were observed between pH 12 and 14 under pseudo-first-order conditions (i.e., when the concentration of CySH was at least 7 times larger than that of $[\text{CyS(=O)SCy}]_0$) (Figure 9). Linear correlations were found for both the pH-dependent and pH-independent reactions, and the linear fits pass through the origin. In a different experiment, when an excess of $[\text{CyS(=O)SCy}]$ was used with respect to $[\text{CySH}]_0$, we have found that the ΔAbs of the first observed reaction (Figure 9, rectangular data point) falls on the calibration curve that was developed for the pH-independent reaction when CyS(=O)SCy was the limiting reagent (Figure 9). This observation validates our assumption that the first reaction that was observed when CyS(=O)SCy was mixed with CySH is the bimolecular reaction of these species.

Kinetics of the Reaction of CyS(=O)SCy with CySH between pH 6 and 14. The rate of the reaction between CyS(=O)SCy and CySH is insensitive to pH between 9.0 and 11.5 (vide supra). However, the rate starts to increase below pH 9. The reaction kinetics exhibit an inflection point with a maximum rate at about pH 7.7, which is indicative of a competitive acid–base equilibrium. The rate decreases below pH 7.7, suggesting that CyS^- , and not CySH^0 , is the reactive

SCHEME 6. Proposed Mechanism, Equilibrium, and Rate Constants (at 18 °C) for the Reaction of CyS(=O)SCy with CySH at $6 < \text{pH} < 10$



species (Schemes 2 and 3).³⁷ The observed increase in the rate below pH 9 suggests that the protonation of the amines of CyS(=O)SCy results in an increase in reactivity. The inflection point of the bell-shaped curve of Figure 2 is located at the average value of the acid dissociation constants for the amine moieties of CyS(=O)SCy (Figure 2: $pK_a^{\text{ester}} = (pK_{a3}^{\text{ester}} + pK_{a4}^{\text{ester}})/2 = (7.3 + 7.9)/2 = 7.6$). Since CyS(=O)SCy reacts as an electrophile, we interpret the increased reactivity of the protonated species as a charge effect. Furthermore, since the observed rate constants continue to decrease below pH 6, CyS^- is still the reaction partner of CyS(=O)SCy under very acidic conditions. Thus, the half-life of the reaction at pH 0 is on the order of hours under the experimental conditions that are given in the caption of Figure 2 (data not shown).

We propose that the various protonated forms of CyS(=O)SCy have different reactivities toward $\text{CyS}^-/\text{CyS}^{2-}$, which gives rise to the four different pathways of Scheme 6 and to the following rate law:

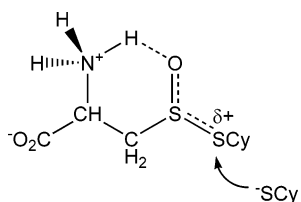
$$\begin{aligned} \text{rate} &= \frac{-d[\text{CyS(=O)SCy}]}{dt} = \\ & \{ K_{a2s}^{\text{CySH}} k_{1b} [\text{H}^+]^3 + K_{a2s}^{\text{CySH}} K_{a3}^{\text{ester}} k_{1b} [\text{H}^+]^2 + \\ & K_{a2s}^{\text{CySH}} K_{a3}^{\text{ester}} K_{a4}^{\text{ester}} k_{1b}'' [\text{H}^+] + K_{a2n}^{\text{CySH}} K_{a3s}^{\text{CySH}} K_{a3}^{\text{ester}} K_{a4}^{\text{ester}} k_{1b}''' \} \times \\ & \frac{[\text{CySH}]_T [\text{CyS(=O)SCy}]_T}{([\text{H}^+]^2 + K_{a3}^{\text{ester}} [\text{H}^+] + K_{a3}^{\text{ester}} K_{a4}^{\text{ester}}) ([\text{H}^+]^2 + \\ & K_{a2n}^{\text{CySH}} [\text{H}^+] + K_{a2s}^{\text{CySH}} [\text{H}^+] + K_{a2n}^{\text{CySH}} K_{a3s}^{\text{CySH}})} \quad (9) \end{aligned}$$

Equation 9 was derived assuming CyS^- is the dominant reacting thiolate below pH 9 (where CyS(=O)SCy^0 and CyS(=O)SCy^- are populated). The solid line in Figure 2 (top) represents the nonlinear least-square fit of the data to eq 9 using $pK_{a2s}^{\text{CySH}} = 8.49$, $pK_{a2n}^{\text{CySH}} = 8.85$, $pK_{a3s}^{\text{CySH}} = 10.00$, $pK_{a3n}^{\text{CySH}} = 10.35$, $pK_{a3}^{\text{ester}} = 7.32$, $pK_{a4}^{\text{ester}} = 7.92$ to produce the following rate constants: $k_{1b} = 4.7(2) \times 10^5 \text{ M}^{-1} \text{ s}^{-1}$, $k_{1b}' = 5.7(6) \times 10^4 \text{ M}^{-1} \text{ s}^{-1}$, $k_{1b}'' = 3.6(7) \times 10^3 \text{ M}^{-1} \text{ s}^{-1}$, and $k_{1b}''' = 4.6(3) \times 10^3 \text{ M}^{-1} \text{ s}^{-1}$.

It is noteworthy that the nucleophilicities of CyS^- and CyS^{2-} toward CyS(=O)SCy^{2-} (i.e., k_{1b}'' and k_{1b}''') are comparable. This is somewhat surprising since one might expect to observe a

(37) Martell, A. E.; Smith, R. M. *Critical Stability Constants*, second supplement, 1989; Vol. 6, p 604.

charge effect for such nucleophilic/electrophilic reactions.^{19,38,39} Perhaps there is a coincidental cancellation of charge effects whereby CyS^{2-} is a better nucleophile, but CyS^- experiences less charge repulsion in its reaction with CyS(=O)SCy^{2-} . In contrast to the insensitivity of the thiolate with respect to charge, the reactivity of CyS(=O)SCy shows a marked sensitivity to the protonation states of its amine groups. Given the magnitude of the reactivity differences of CyS(=O)SCy^0 and CyS(=O)SCy^- versus CyS(=O)SCy^{2-} , it appears likely to us that the increase in reactivity that is observed upon protonation of the amine groups is a consequence of specific acid catalysis, perhaps *vis-à-vis* an intramolecular hydrogen bond:



We note that Kice et al. have previously observed acid catalysis of nucleophilic reactions of aromatic thiosulfinate esters.⁴⁰

A Comparison of the Different Methods of Generating CySOH. Scheme 4 summarizes possible reactions of CySOH with the five redox derivatives that we have considered in this contribution. The opposite reactions can potentially offer methods of generating CySOH. We have shown in a previous study that hydrolysis of CyS(=O)SCy is too slow to permit the study of CySOH (Scheme 4, **1a**),¹⁹ and we report herein that hydrolysis of CySSCy (Scheme 4, **-2**) is even slower. The present study exploits the facile reaction of CyS(=O)SCy with CySH (Scheme 4, **1b**) at high pH to generate CySOH. The reaction of $\text{CyS(=O)}_2\text{SCy}$ with CySH (Scheme 4, **-1d**) remains unexplored. However, an alternative approach to generating CySOH *in situ* is the oxidation of CySH by reactions that are capable of delivering an oxygen atom. Sluggish oxidants like hydrogen peroxide are ineffective for producing CySOH at a sufficient rate for studying the subsequent reactions.^{41,42} However, we have recently discovered that CySOH can be generated by the facile reaction of CySH with hypohalous acids (HOX, X = Cl or Br).³⁴ As forecasted in the data presented in Figure 3, the reaction mechanisms that are associated with the latter reaction are consistent with the present study.

Conclusions

The reaction of CyS(=O)SCy with CySH produces CySSCy and the reactive species CySOH. Above pH 12, this reaction is sufficiently facile that the subsequent comproportionation of CySOH with CySH can be observed. We report herein an investigation of the latter reaction, which is apparently the first detailed mechanistic study of a reaction of CySOH. Unfortunately, the resulting kinetics can only be described in terms of the variable K_a^{CySOH} of the sulfenic acid moiety of CySOH (because the value of the acid dissociation constant for CySOH apparently lies below pH 12). In a parallel study, we have

investigated the oxidation of CySH with HOX (X = Cl, Br), which is a more facile means of generating CySOH.³⁴ This reaction has allowed us to extend the pH range downward to further explore the chemistry of CySOH.³⁴

Experimental Section

Reagents. All chemicals were A.C.S. certified grade or better. Water was doubly distilled in glass. Solutions of NaOH, mostly free of CO_2 contamination, were quantified by titration with potassium hydrogen phthalate or standardized HCl, HClO_4 solutions using phenolphthalein as an indicator. HClO_4 and HCl were standardized against bicarbonate. The buffer solutions were prepared from the solids K_3PO_4 , $\text{NaH}_2\text{PO}_4 \cdot \text{H}_2\text{O}$, Na_2HPO_4 , and $\text{Na}_3\text{PO}_4 \cdot 12\text{H}_2\text{O}$; the ionic strength was adjusted with NaClO_4 ; and the pH/pD was adjusted with NaOH, NaOD, HClO_4 , or DCl. L-Cysteine, L-cystine, L-cysteinesulfinic acid monohydrate, L-cysteic acid monohydrate, peracetic acid, deuterium chloride (35 wt % solution in D_2O), NaOD (40 wt % solution in D_2O), NaClO_4 , K_3PO_4 , $\text{NaH}_2\text{PO}_4 \cdot \text{H}_2\text{O}$, Na_2HPO_4 , and $\text{Na}_3\text{PO}_4 \cdot 12\text{H}_2\text{O}$ were used as received. The synthesis of CyS(=O)SCy was accomplished using a published procedure.⁴³

pH/pD Measurements. The $[\text{OH}^-]$ for the unbuffered solutions was determined by acid–base titration against standardized HCl or standardized HClO_4 solutions. The $[\text{H}^+]$ of the buffered solutions was determined with an ion analyzer using a Ag/AgCl combination pH electrode. The ionic strength was kept constant at 1.0 M for all H_2O solutions ($\text{NaClO}_4 + \text{NaOH/HClO}_4 + \text{iP/Tris}$). To obtain the $[\text{H}^+]$ or $[\text{OH}^-]$ of the buffered solutions from the measured pH values, all pH measurements were corrected for the “Irving factor”⁴⁴ and the ionic product of water (pK_w) that were measured by titration of a 1.0 M NaClO_4 solution by a standardized solution of 0.1 M NaOH (in 1.0 M NaClO_4); pD measurements in D_2O were made using the same pH electrode by adding 0.4 units to the measurement.⁴⁵

NMR Studies. ^1H NMR spectra were recorded at $20(\pm 0.5)^\circ\text{C}$. Deuterated buffers were prepared from D_2O solutions of anhydrous K_3PO_4 by adding DCl, by dilution of a 40 wt % NaOD solution with D_2O , or by dilution of a 35 wt % DCl solution with D_2O . The chemical shifts (parts per million) were referenced to sodium 2,2-dimethyl-2-silapentane-5-sulfonate (DSS, $\delta = 0.015$ ppm). Turbulent mixing of reagents was necessary to ensure homogeneity of the reaction mixtures in the time frame of the chemical reactions, and this was achieved for the NMR studies by employing a hand mixer comprising two gastight syringes and a T-mixer. Failure to quickly mix solutions produced different, irreproducible results.

UV/Vis Spectroscopy. Electronic spectra were measured using a diode array spectrophotometer using quartz cells with calibrated 1 mm, 2 mm, and 1 cm path lengths at 20°C or the monochromator of the stopped-flow instrument with a 1 cm path length using a Xe arc lamp and a PMT detector at 18°C .

General Description of the Stopped-Flow Studies. Kinetic measurements were made with a stopped-flow spectrophotometer using a Xe arc lamp and a PMT detector. A double-mixing mode was used for some of the experiments. All the stopped-flow measurements were made at a temperature of 18°C maintained in the observation cell with a circulator. The adiabatic temperature increases that were associated with the pH-jump experiments were determined experimentally to be less than 1°C .

Reaction of CyS(=O)SCy with CySH. The pH and $[\text{CySH}]$ dependencies of the reaction rates were investigated under pseudo-first-order conditions using excess $[\text{CySH}]$ over $[\text{CyS(=O)SCy}]$

(38) Nagy, P.; Ashby, M. T. *Chem. Res. Toxicol.* **2005**, *18*, 919–923.

(39) Nagy, P.; Ashby, M. T. *Chem. Res. Toxicol.* **2007**, *20*, 79–87.

(40) Kice, J. J.; Cleveland, J. P. *J. Am. Chem. Soc.* **1970**, *92*, 4757–4758.

(41) Ashby, M. T.; Nagy, P. *J. Pharm. Sci.* **2005**, *95*, 15–18.

(42) Ashby, M. T.; Nagy, P. *Int. J. Chem. Kinet.* **2006**, *39*, 32–38.

(43) Walti, M.; Hope, D. B. *J. Chem. Soc., Perkin Trans. 1* **1971**, *12*, 2326–2328.

(44) Irving, H. M. N. H.; Miles, M. G.; Pettit, L. D. *Anal. Chim. Acta* **1967**, *38*, 475–488.

(45) Glasoe, P. K.; Long, F. A. *J. Phys. Chem.* **1960**, *64*, 188–190.

in single-mixing stopped-flow experiments. The concentration of H^+ ions in the $CyS(=O)SCy$ solutions before mixing was kept at 0.5 M to suppress the rate of hydrolysis of $CyS(=O)SCy$. The pH of the $CyS(=O)SCy/CySH$ reaction mixtures were adjusted in situ by introducing the appropriate amount of NaOH and iP or Tris to the $CySH$ solutions. All solutions were kept in the dark, and no autoxidation of $CySH$ could be detected by 1H NMR even at very high pH. Equal amounts of $NaClO_4$ were added to the $CyS(=O)SCy$ and $CySH$ solutions to set the ionic strength of the reaction mixture to 1.0 M after the pH-jump. The efficiency of mixing in the single-mixing experiments was confirmed by repeating the experiments in double-mixing mode. The pH of the $CyS(=O)SCy$ solutions was adjusted in the first mixing cycle by mixing with the appropriate buffer ($NaOH + iP/Tris + NaClO_4$) followed by mixing with $CySH$ in the second mixing cycle after a delay time of 0.05 s. No significant hydrolysis occurs in this time frame. Essentially the same rate constants were observed by the two different mixing sequences. The effect of $[CySSCy]$ on the reactions of $CySH$ with $CyS(=O)SCy$ and with $CySOH$ was studied using double-mixing

stopped-flow experiments that were similar to those described above, where different amounts of $CySSCy$ were added to the $CySH$ solutions.

Kinetic Data Analysis. The monochromatic kinetic traces were fit with KinetAsyst 3.14 software (Hi-Tech, UK). Polychromatic data were analyzed using SPECFIT/32 (Spectrum Software Associates), a multivariate data analysis program. The concentration dependencies of the pseudo-first-order rate constants were obtained by linear least-squares fits of the data with KaleidaGraph 3.6 (Synergy Software) or Mathematica (Wolfram Research, Version 5.2).

Acknowledgment. We appreciate the financial support we have received from the National Science Foundation (CHE-0503984), the American Heart Association (0555677Z), the Petroleum Research Fund (42850-AC4), and the National Institutes of Health (1 R21 DE016889-01A2).

JO701813F